Electronic Supplementary Information (ESI) for

Bright and Stable Quaternary Ammonium Antinomy Halides for Solid-State Lighting

*Shiqi Sui, Chuying Wang, Guangcai Hu, Yacong Li, Wen Meng, Jingwei Luo, Guangyong Xu, and Zhengtao Deng**

College of Engineering and Applied Sciences, State Key Laboratory of Analytical Chemistry for Life Science, National Laboratory of Microstructures, Nanjing University, Nanjing, Jiangsu 210023, P. R. China.

E-mail: dengz@nju.edu.cn

Experimental Section

Materials

Antimony trichloride ($SbCl_3$, 99 %, Alfa Aesar), octyltrimethylammonium chloride ($[C_8H_{17}(CH_3)_3]NCl$, 98 %, Heowns), decyltrimethylammonium chloride ($[C_{10}H_{21}(CH_3)_3]NCl$, 98 %, Heowns), dodecyltrimethylammonium chloride ($[C_{12}H_{25}(CH_3)_3]NCl$, 97 %, Heowns), tetradecyltrimethylammonium chloride ($[C_{14}H_{29}(CH_3)_3]NCl$, 99%, Heowns), hexadecyltrimethylammonium chloride ($[C_{16}H_{33}(CH_3)_3]NCl$, 98%, Aladdin), octadecyltrimethylammonium chloride ($[C_{18}H_{37}(CH_3)_3]NCl$, 98 %, Heowns), docosyltrimethylammonium chloride ($[C_{22}H_{45}(CH_3)_3]NCl$, 80 %, Adamas), N,N-Dimethylformamide (DMF, Sinopharm Chemical Reagent Co., Ltd), dimethyl sulfoxide (DMSO, Sinopharm Chemical Reagent Co., Ltd), ethyl ether (Et_2O, Nanjing Reagent), Toluene (AR, Aladdin), Polystyrene(PS, commercial), $BaMgAl_{10}O_{17}$: Eu (BAM blue phosphor, commercial, Shenzhen Looking Long Technology Co., Ltd), $(Sr, Ba)_2SiO_4$: Eu (Silicates green phosphor, commercial, Shenzhen Looking Long Technology Co., Ltd), $(Sr, Ba)AlSiN_3$: Eu (Nitrides red phosphor, commercial, Shenzhen Looking Long Technology Co., Ltd)

Synthesis of $[C_xH_{2x+1}(CH_3)_3N]_2SbCl_5$

For a typical synthesis of $[C_8H_{17}(CH_3)_3N]_2SbCl_5$, 0.1 mmol $[C_8H_{17}(CH_3)_3]NCl$ was dissolved in 10 ml DMF by sonication until the ammonium chloride was dissolved completely. Subsequently, 0.05 mmol $SbCl_3$ powder was added to the precursor solution. After being dissolved under sonication, 50 ml Et_2O was added to the solution, and a white precipitate appeared rapidly. The suspension was centrifuged at 10000 rpm for 5 min. The supernatant was removed, and the precipitate was washed with DMF and Et_2O for three times to remove the unreacted precursors. The finally products were dried under vacuum overnight for further characterizations. The synthesis processes of $[C_xH_{2x+1}(CH_3)_3N]_2SbCl_5$ (x = 10/12/14/16/18/22) were the similar as the method mentioned above, but $[C_8H_{17}(CH_3)_3]NCl$ was changed to $[C_xH_{2x+1}(CH_3)_3]NCl$ (x = 10/12/14/16/18/22), and the volume of DMF was adjusted to dissolve all the solid raw materials.

LED fabrication

For a typical fabrication of orange-light LED, a specific weight of $[C_{16}H_{33}(CH_3)_3N]_2SbCl_5$ phosphor is blended well with 75% PS toluene solution. The blended phosphor of PS paste is daubed on the surface of the InGaN UV LED chips (365–370 nm) and dried in an oven under vacumm for 2 hours. Similarly, the white-light LEDs are fabricated in the same process, but the phosphor is replaced by mixed phosphors, which contain BAM blue phosphor, silicate green phosphor, and $[C_{16}H_{33}(CH_3)_3N]_2SbCl_5$ as the orange phosphor.

Characterizations

Powder XRD is measured with a Bruker D8 ADVANCE X-ray Diffractometer equipped with monochromatized Cu Kα radiation (λ = 1.5418 Å). The diffraction patterns are scanned over the angular range of 5 ° ~ 50 ° (2θ) with the step length of 0.02 ° at room temperature. Scanning electron microscopy (SEM) is performed on a ZEISS Ultra 55 electron microscope operating at 10 kV equipped with Oxford Inca X-MAX energy-dispersive X-ray spectroscopy (EDS) detector. TG is collected with NETZSCH thermalgravimetric analyzer and the testing range is from room temperature to 500 °C. DSC is collected with NETZSCH differential scanning calorimeter and the testing range is from room temperature to 500 °C. The photoluminescence (PL) spectra are carried out with a Horiba PTI QuantaMaster 400 steady-state fluorescence system or with a fiber fluorimeter system from Thorlabs operating under ambient conditions. UV-vis spectra are recorded with a Shimadzu UV-3600 plus spectrophotometer equipped with an integrating sphere under ambient conditions. The absolute fluorescence quantum yields are measured using a Horiba PTI QuantaMaster 400 steady-state fluorescence system with an integrated sphere and double-checked with a Hamamatsu Photonics Quantaurus-QY (model: C11347-11) under ambient conditions. Time-resolved PL emission decay curves are collected at room temperature and detected by Edinburgh FLS-980 steady-state fluorescence spectrometers with a 365 nm picosecond laser under ambient conditions. The photoelectric properties, including the emission spectra, CCT, luminous efficiency, and CIE color coordinates of LEDs are collected with an integrating sphere spectroradiometer system (HP8000, Hangzhou ICE Instrument) under ambient conditions. All the independent experiments are done three times and the test errors of the results are below 1%.

Additional Figures:

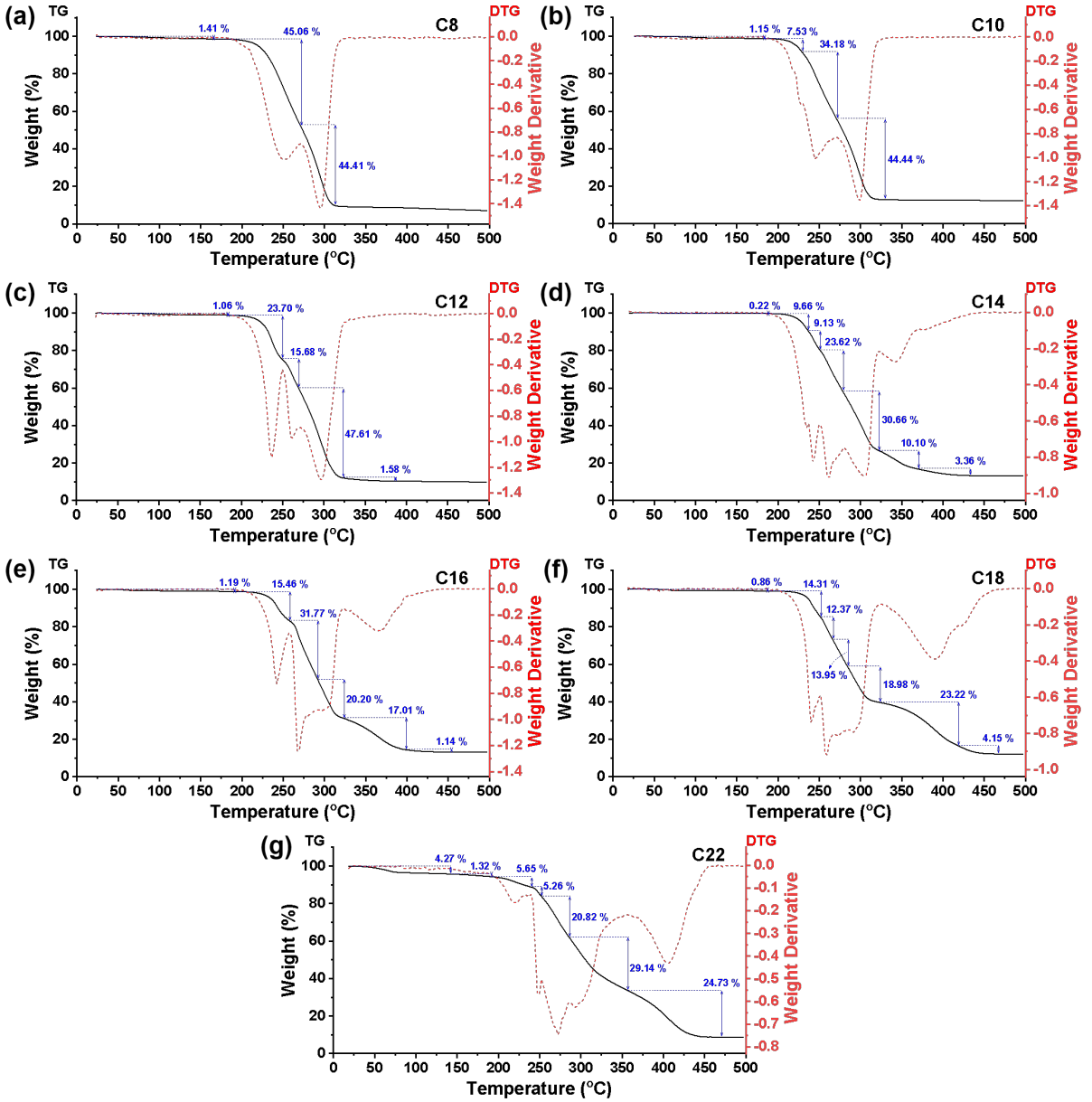

Figure S1. TG curves (black solid lines) and DTG curves (red dash lines) of $[C_xH_{2x+1}(CH_3)_3N]_2SbCl_5$. Weight-loss percentages and corresponding ranges are marked with blue dotted lines and arrows in each figure.

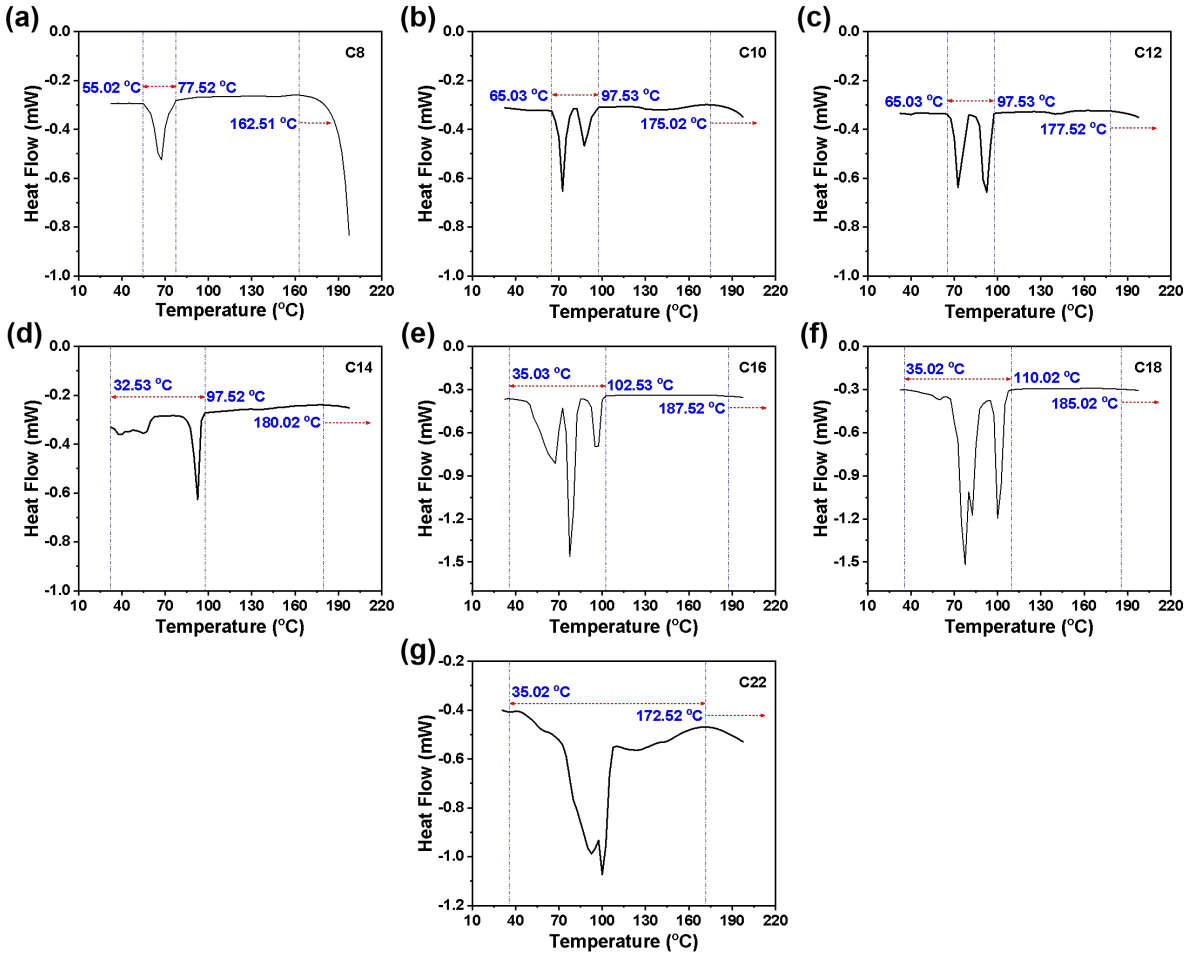

Figure S2. DSC curves of $[C_xH_{2x+1}(CH_3)_3N]_2SbCl_5$. The endothermic ranges are marked with blue dash lines and red arrows. The beginning and ending temperatures of the endothermic process are listed in each figure.

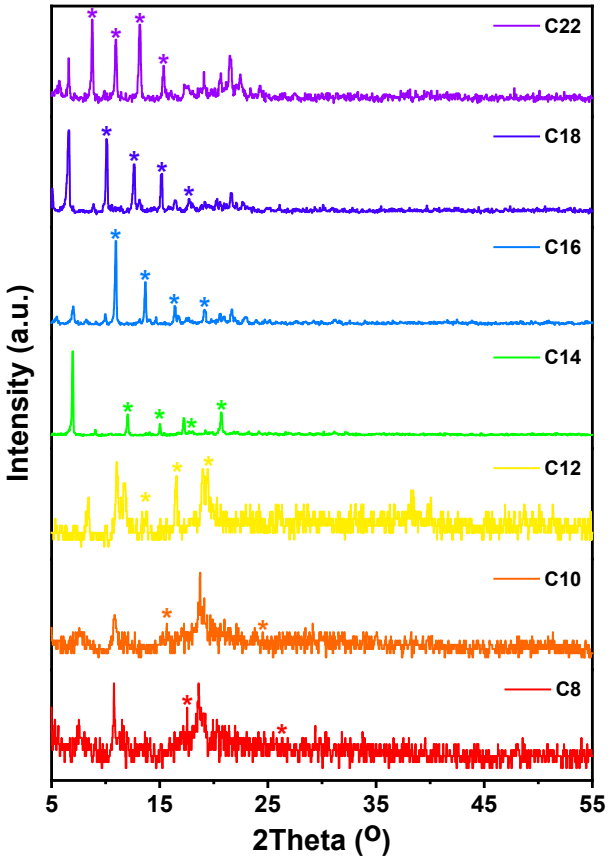

Figure S3. XRD patterns of $[C_xH_{2x+1}(CH_3)_3N]_2SbCl_5$ (x = 8/10/12/14/16/18/22). The specific peaks are marked with stars.

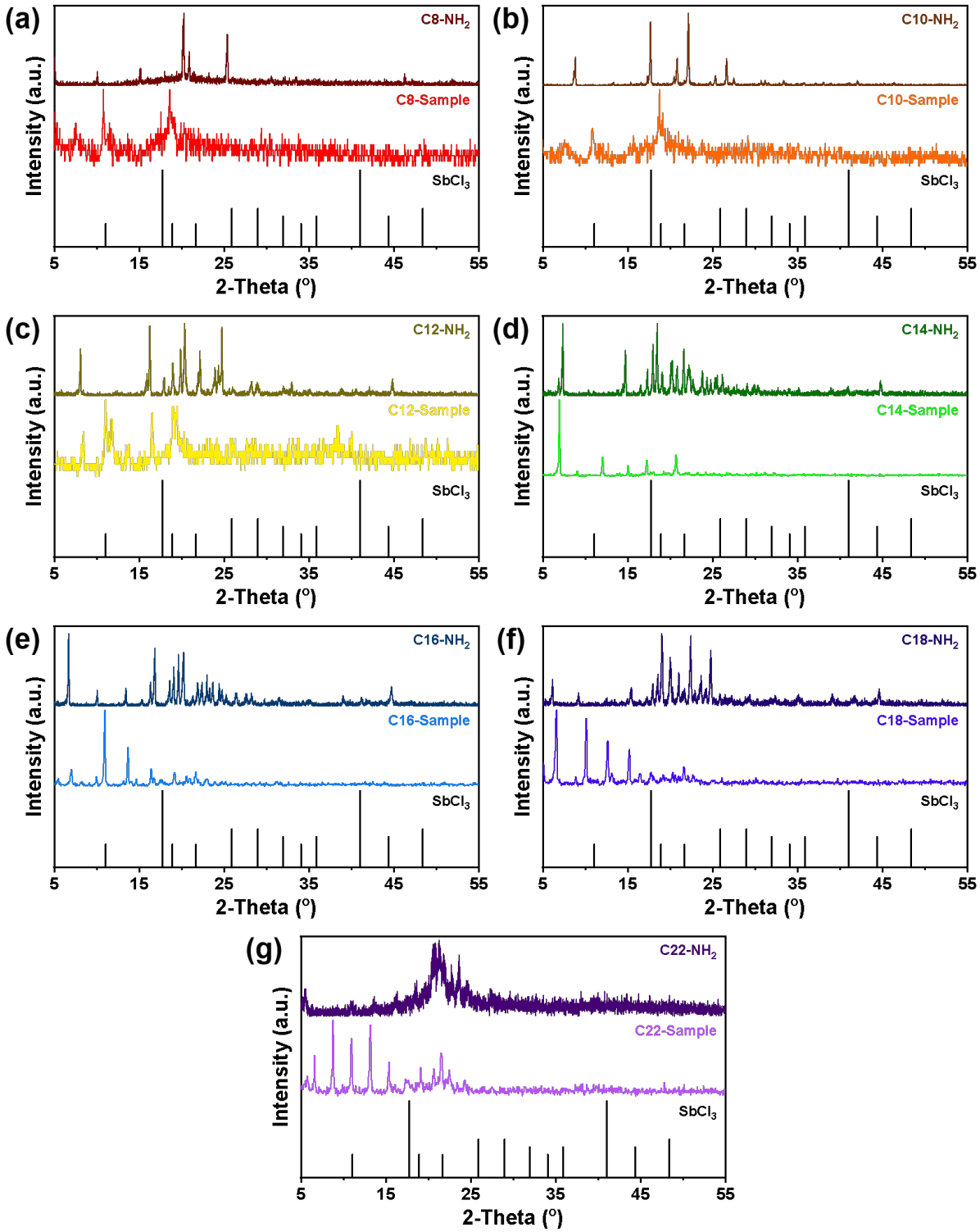

Figure S4. The powder XRD patterns of $[C_xH_{2x+1}(CH_3)_3N]_2SbCl_5$ and corresponding raw materials. Patterns of $SbCl_3$ are from standard PDF cards (PDF# 01–0248). Patterns of organic ammonium hydrochloride are from experimental data. In each figure, the powder XRD patterns of the sample are marked by "Cx-Sample" with light colors, and corresponding organic ammonium salts are marked by "Cx-NH_2" with deep colors.

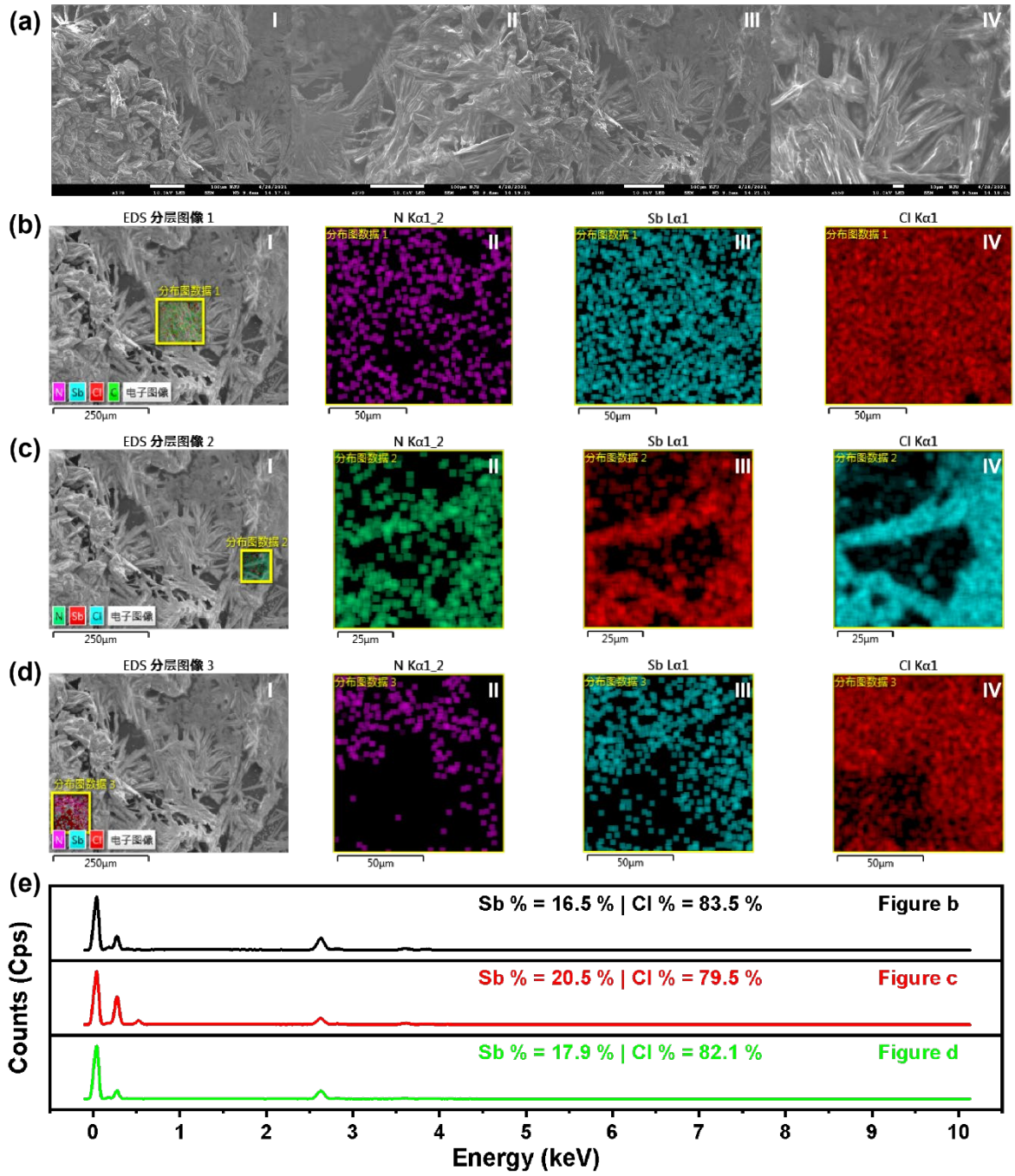

Figure S5. (a) SEM images of $[C_8H_{17}(CH_3)_3N]_2SbCl_5$. (b–e) EDS mapping images of $[C_8H_{17}(CH_3)_3N]_2SbCl_5$. In each group, Figure I refers to the SEM images, in which the yellow square is the analyzed area of the element. Figure II is the distribution image of N mapping. Figure III is the distribution image of Sb mapping. Figure IV is the distribution image of Cl mapping. Corresponding elements are listed above the figures. (f) The spectra corresponding to the EDS mapping are shown in Figures b–d. The corresponding EDS images are marked on the upper right of the spectra, while the ratios and types of elements are listed in each figure.

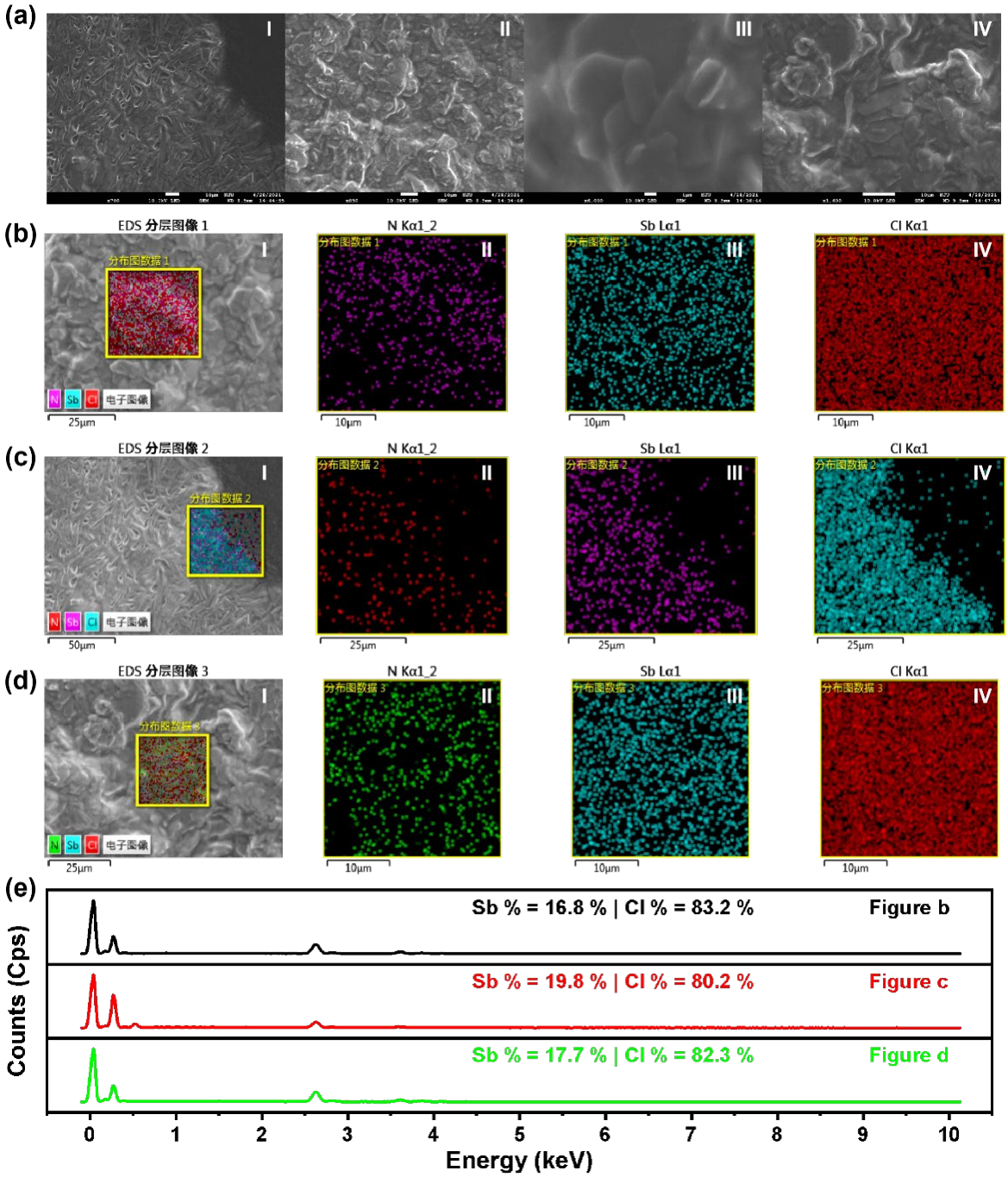

Figure S6. (a) SEM images of $[C_{10}H_{21}(CH_3)_3N]_2SbCl_5$. (b–e) EDS mapping images of $[C_{10}H_{21}(CH_3)_3N]_2SbCl_5$. In each group, Figure I refers to the SEM images, in which the yellow square is the analyzed area of the element. Figure II is the distribution image of N mapping. Figure III is the distribution image of Sb mapping. Figure IV is the distribution image of Cl mapping. Corresponding elements are listed above the figures. (f) The spectra corresponding to the EDS mapping are shown in Figures b–d. The corresponding EDS images are marked on the upper right of the spectra, while the ratios and types of elements are listed in each figure.

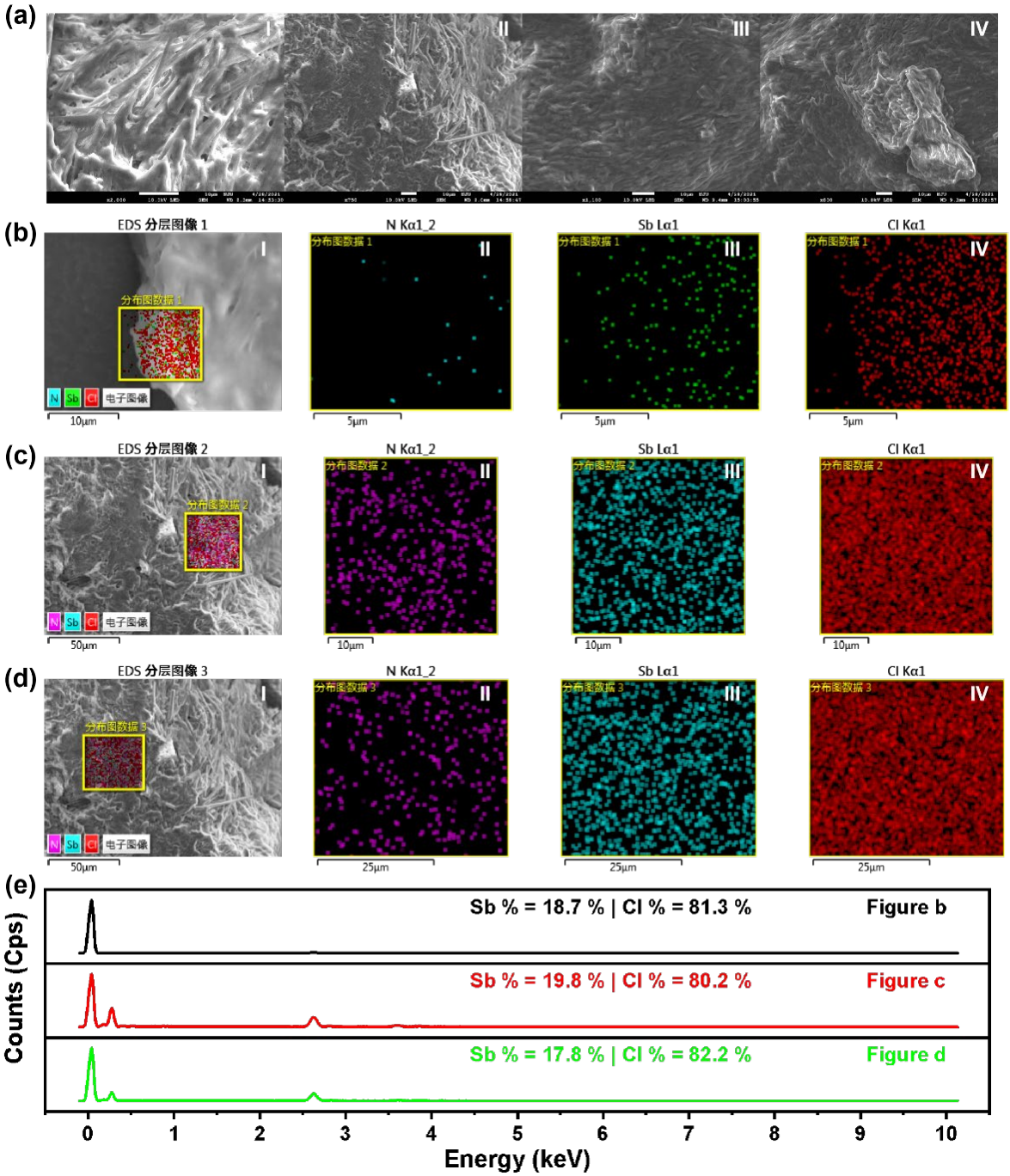

Figure S7. (a) SEM images of $[C_{12}H_{25}(CH_3)_3N]_2SbCl_5$. (b–e) EDS mapping images of $[C_{12}H_{25}(CH_3)_3N]_2SbCl_5$. In each group, Figure I refers to the SEM images, in which the yellow square is the analyzed area of the element. Figure II is the distribution image of N mapping. Figure III is the distribution image of Sb mapping. Figure IV is the distribution image of Cl mapping. Corresponding elements are listed above the figures. (f) The spectra corresponding to the EDS mapping are shown in Figures b–d. The corresponding EDS images are marked on the upper right of the spectra, while the ratios and types of elements are listed in each figure.

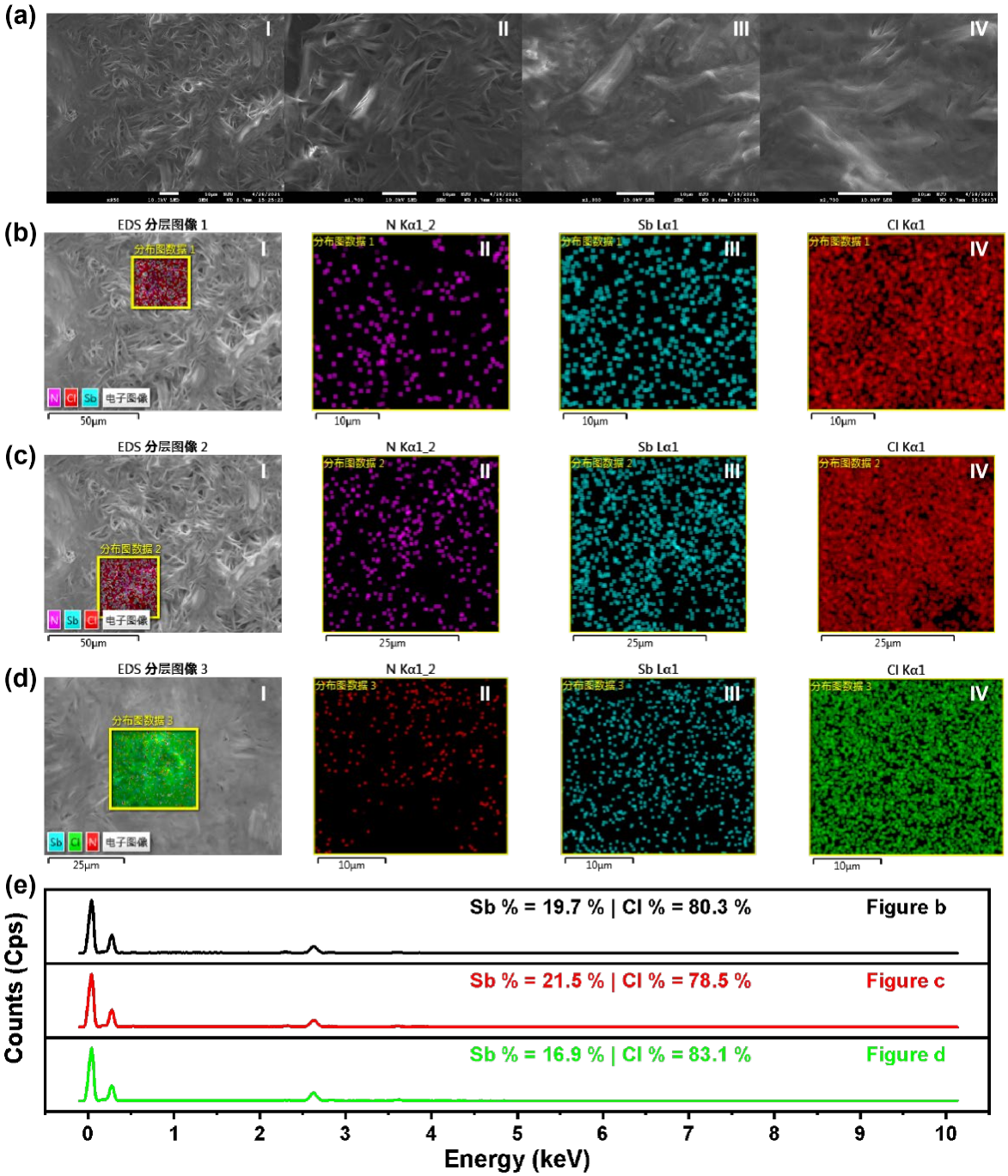

Figure S8. (a) SEM images of $[C_{14}H_{29}(CH_3)_3N]_2SbCl_5$. (b-e) EDS mapping images of $[C_{14}H_{29}(CH_3)_3N]_2SbCl_5$. In each group, Figure I refers to the SEM images, in which the yellow square is the analyzed area of the element. Figure II is the distribution image of N mapping. Figure III is the distribution image of Sb mapping. Figure IV is the distribution image of Cl mapping. Corresponding elements are listed above the figures. (f) The spectra corresponding to the EDS mapping are showed in Figures b–d) The corresponding EDS images are marked on the upper right of the spectra, while the ratios and types of elements are listed in each figure.

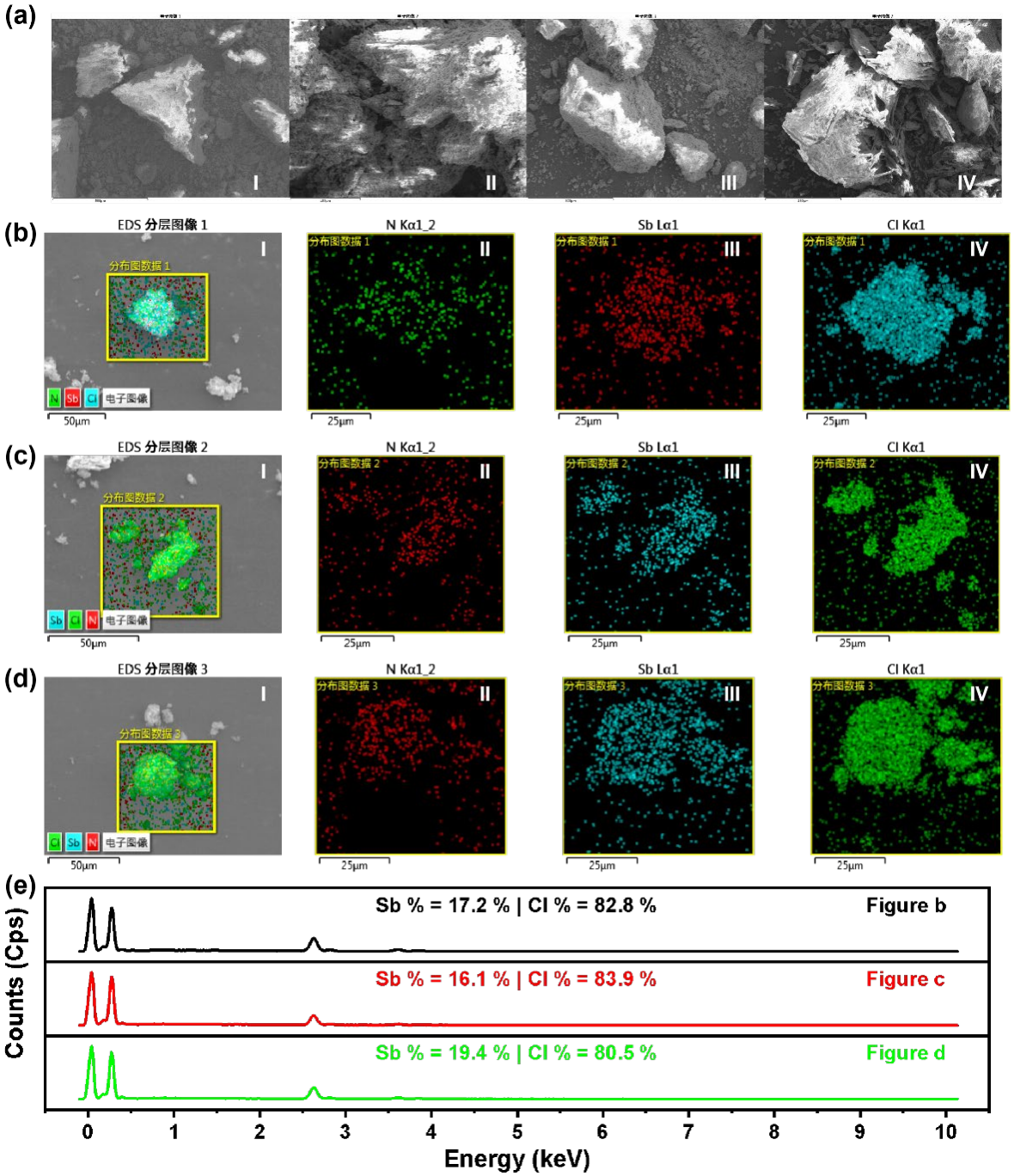

Figure S9. (a) SEM images of $[C_{16}H_{33}(CH_3)_3N]_2SbCl_5$. (b-e) EDS mapping images of $[C_{16}H_{33}(CH_3)_3N]_2SbCl_5$. In each group, Figure I refers to the SEM images, in which the yellow square is the analyzed area of the element. Figure II is the distribution image of N mapping. Figure III is the distribution image of Sb mapping. Figure IV is the distribution image of Cl mapping. Corresponding elements are listed above the figures. (f) The spectra corresponding to the EDS mapping are shown in Figures b–d. The corresponding EDS images are marked on the upper right of the spectra, while the ratios and types of elements are listed in each figure.

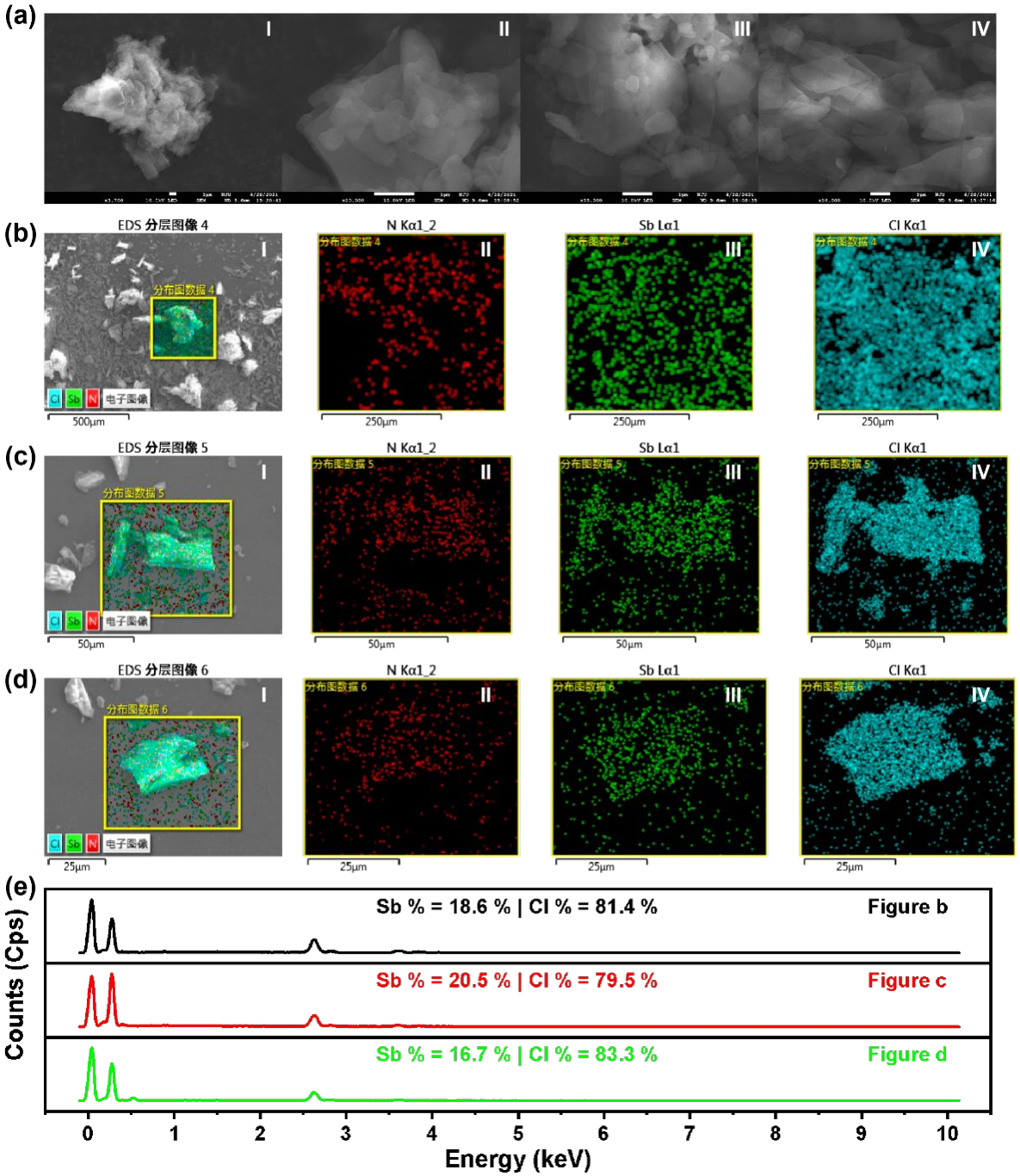

Figure S10. (a) SEM images of $[C_{18}H_{37}(CH_3)_3N]_2SbCl_5$. (b-e) EDS mapping images of $[C_{18}H_{37}(CH_3)_3N]_2SbCl_5$. In each group, Figure I refers to the SEM images, in which the yellow square is the analyzed area of the element. Figure II is the distribution image of N mapping. Figure III is the distribution image of Sb mapping. Figure IV is the distribution image of Cl mapping. Corresponding elements are listed above the figures. (f) The spectra corresponding to the EDS mapping are showed in Figures b–d. The corresponding EDS images are marked on the upper right of the spectra, while the ratios and types of elements are listed in each figure.

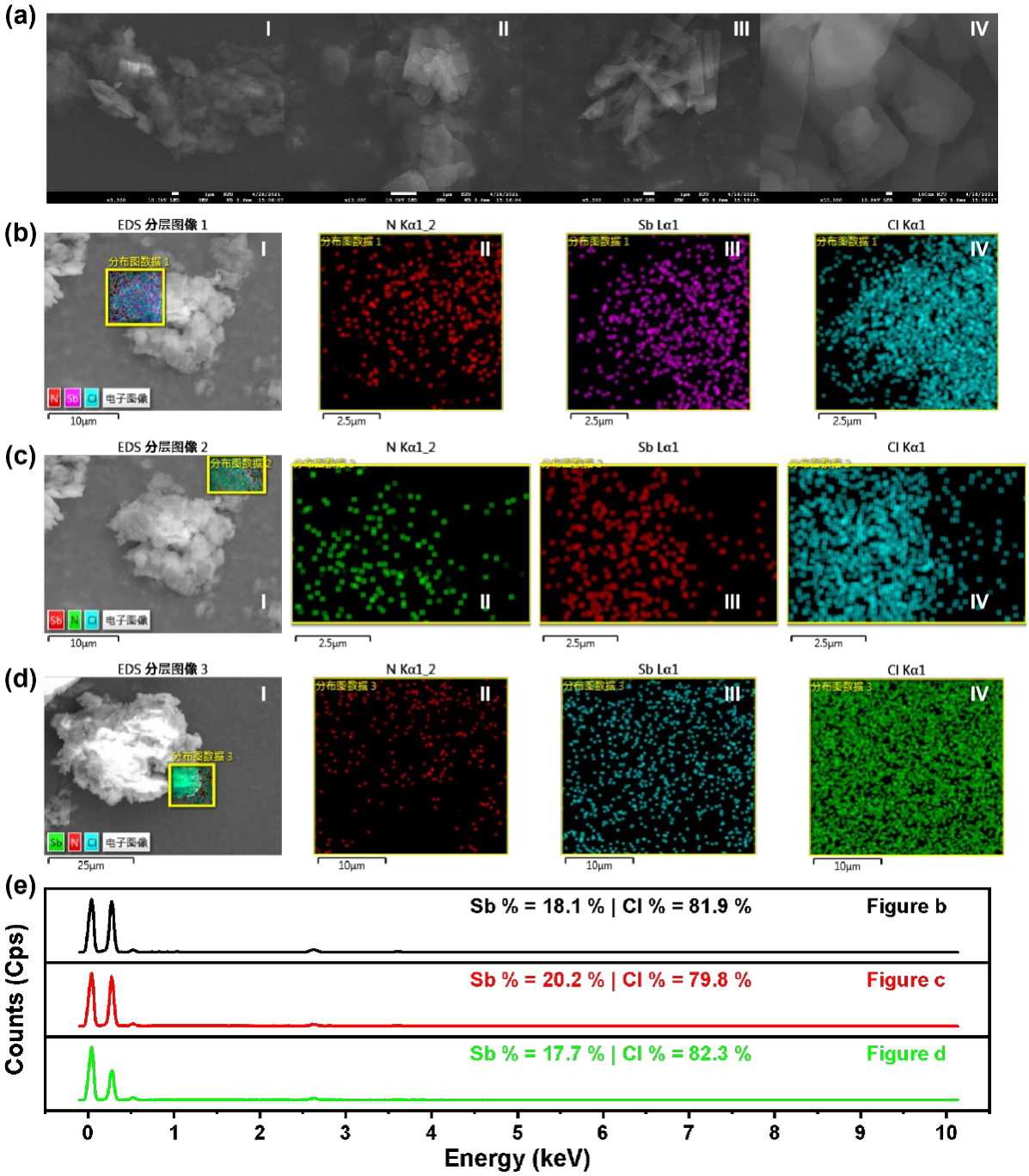

Figure S11. (a) SEM images of $[C_{22}H_{45}(CH_3)_3N]_2SbCl_5$. (b-e) EDS mapping images of $[C_{22}H_{45}(CH_3)_3N]_2SbCl_5$. In each group, Figure I refer to the SEM images, in which the yellow square is the analysed area of the element. Figure II is the distribution image of N mapping. Figure III is the distribution image of Sb mapping. Figure IV is the distribution image of Cl mapping. Corresponding elements are listed above the figures. (f) The spectra corresponding to the EDS mapping are showed in Figures b–d. The corresponding EDS images are marked on the upper right of the spectra, while the ratios and types of elements are listed in each figure.

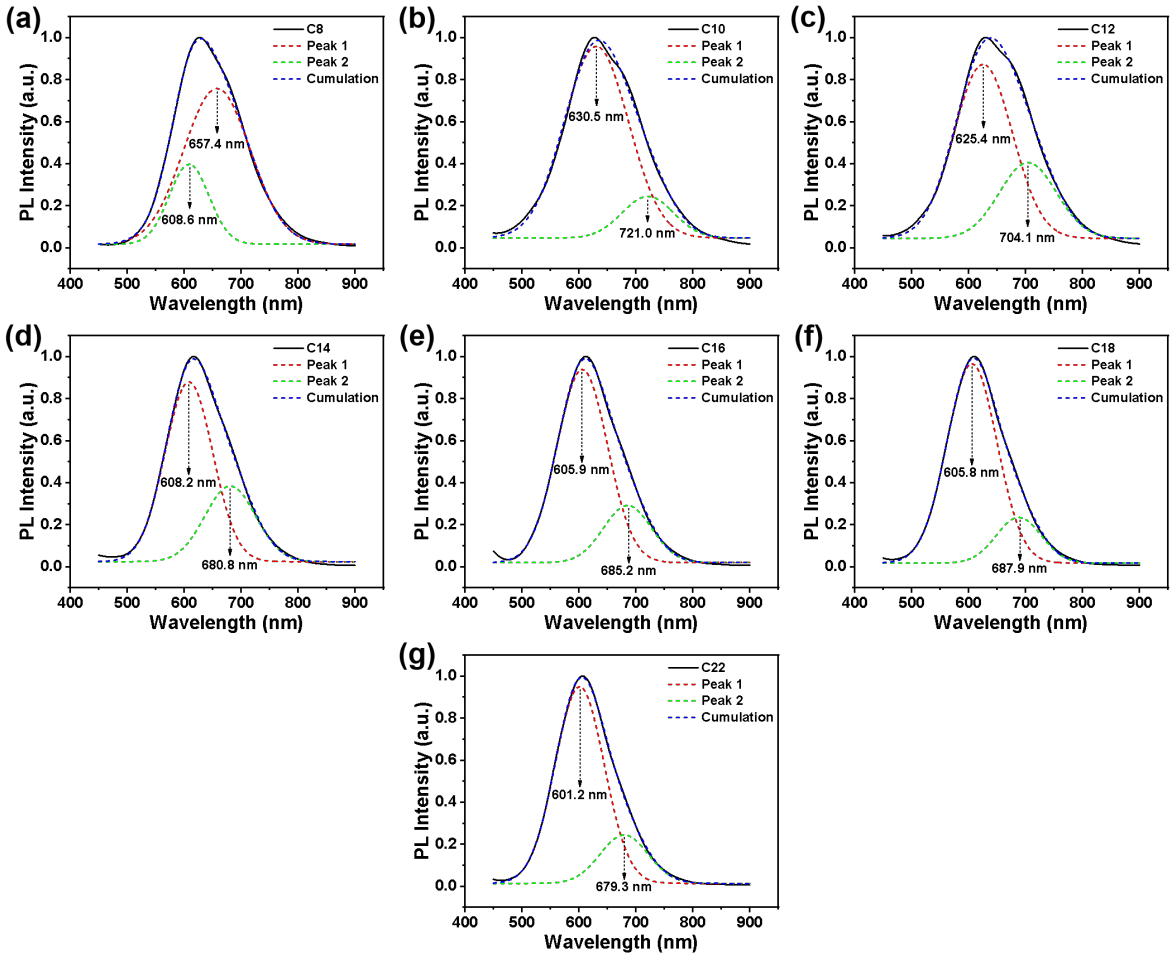

Figure S12. The differentiated–fitting results and peak positions of the emission peaks of $[C_xH_{2x+1}(CH_3)_3N]_2SbCl_5$ with different A-site cations. Black solid lines indicate original emission peak, red and green dash lines indicate fitting peaks, while blue dash lines indicate the overlapping results of the fitting peaks.

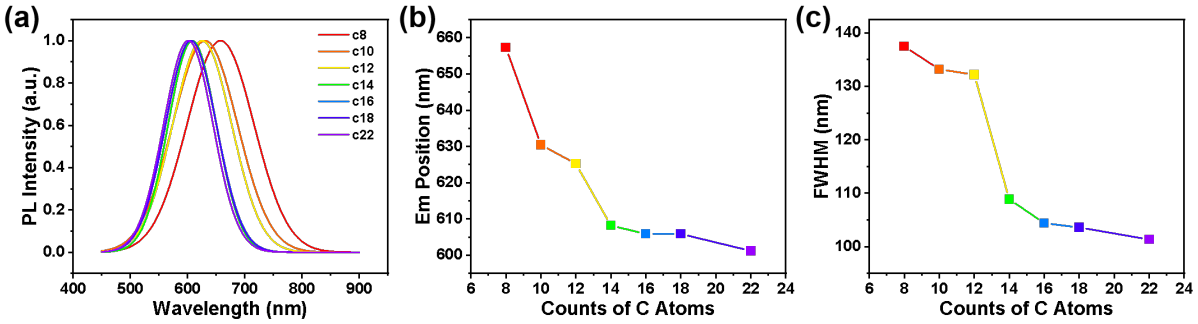

Figure S13. (a) The emission spectra of main peaks from $[C_xH_{2x+1}(CH_3)_3N]_2SbCl_5$–fitted spectra with different A-site cations. (b) Positions of main emission peaks from $[C_xH_{2x+1}(CH_3)_3N]_2SbCl_5$–fitted spectra with different A-site cations. (c) FWHM of main emission peaks from $[C_xH_{2x+1}(CH_3)_3N]_2SbCl_5$–fitted spectra with different A-site cations.

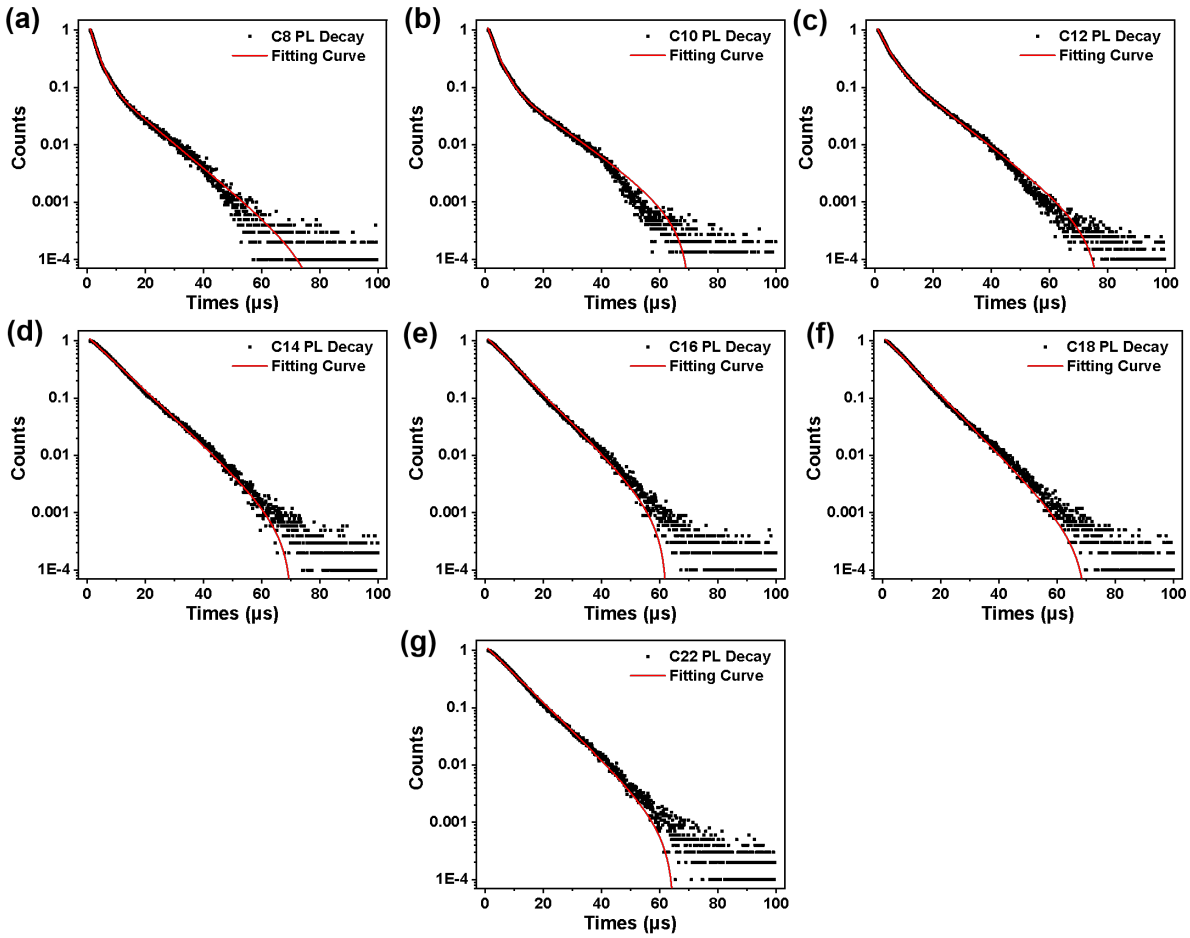

Figure S14. The photoluminescence decay (PL Decay) and fitting curves of $[C_xH_{2x+1}(CH_3)_3N]_2SbCl_5$ with different A-site cations. Black dots indicate the PL decay spectra, while red lines indicate the fitting curves (a–c: single-exponential fitting, d–g: double-exponential fitting).

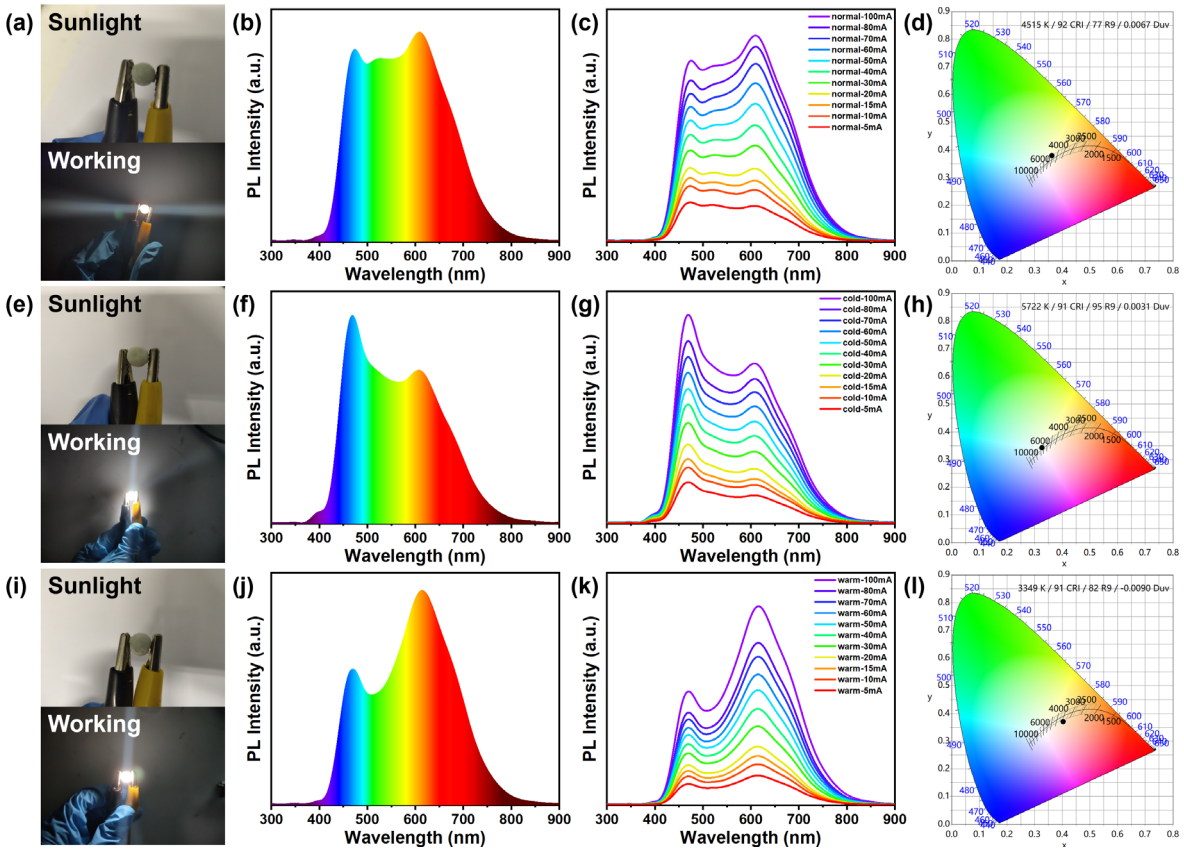

Figure S15. The (a) images of normal-white LED, (e) cold-white LED, and (i) warm-white LED under sunlight and working conditions. The PL spectra with visible light spectra of (b) normal-white LED, (f) cold-white LED, and (j) warm-white LED. The PL spectra under different working currents of (c) normal-white LED, (g) cold-white LED, and (k) warm-white LED. The CIE coordinates of (d) normal-white LED, (h) cold-white LED, and (l) warm-white LED.

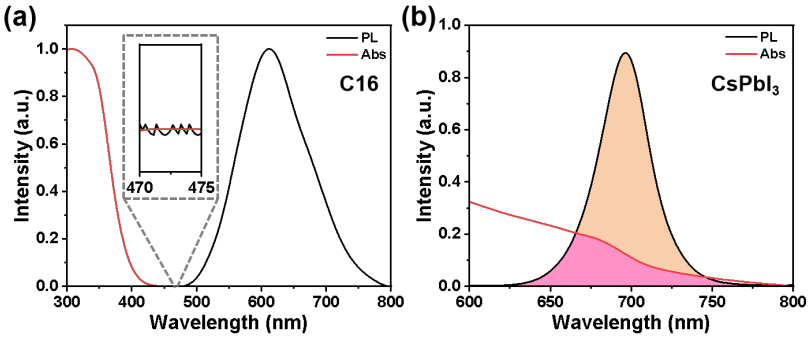

Figure S16. (a) The PL (black line) and absorption (red line) spectra of $[C_{16}H_{33}(CH_3)_3N]_2SbCl_5$. The inset figure is the PL (black line) and absorption (red line) line spectra of $[C_{16}H_{33}(CH_3)_3N]_2SbCl_5$ between 470 ~ 475 nm. (b) The PL (black line) and absorption (red line) spectra of $CsPbI_3$ nanocrystals. These results indicate that the re-absorption of the Sb-halide sample are much less than that of the lead halide samples.

Additional Supporting Tables:

Table S1. Element ratio of $[C_xH_{2x+1}(CH_3)_3N]_2SbCl_5$ from EDS mapping

Samples	Sb : Cl
$[C_8H_{17}(CH_3)_3N]_2SbCl_5$	1 : 4.46
$[C_{10}H_{21}(CH_3)_3N]_2SbCl_5$	1 : 4.52
$[C_{12}H_{25}(CH_3)_3N]_2SbCl_5$	1 : 4.32
$[C_{14}H_{29}(CH_3)_3N]_2SbCl_5$	1 : 4.15
$[C_{16}H_{33}(CH_3)_3N]_2SbCl_5$	1 : 4.69
$[C_{18}H_{37}(CH_3)_3N]_2SbCl_5$	1 : 4.37
$[C_{22}H_{45}(CH_3)_3N]_2SbCl_5$	1 : 4.35

Table S2. Diffraction data with the characteristic peak (theta) and interplanar spacing of different samples.

Samples	Specific peak positions / °				Average interplaner spacing / nm
	2 theta - 1	2 theta - 2	2 theta - 3	2 theta - 4	
$[C_8H_{17}(CH_3)_3N]_2SbCl_5$	17.54	/	/	26.5	3.013996345
$[C_{10}H_{21}(CH_3)_3N]_2SbCl_5$	15.66	/	/	24.5	3.045295702
$[C_{12}H_{25}(CH_3)_3N]_2SbCl_5$	13.77	16.58	19.58	/	3.076656599
$[C_{14}H_{29}(CH_3)_3N]_2SbCl_5$	12.01	15.05	17.71	20.66	3.106236342
$[C_{16}H_{33}(CH_3)_3N]_2SbCl_5$	10.96	13.71	16.37	19.15	3.265752415
$[C_{18}H_{37}(CH_3)_3N]_2SbCl_5$	10.11	12.67	15.19	17.71	3.51385191
$[C_{22}H_{45}(CH_3)_3N]_2SbCl_5$	8.73	10.92	13.19	15.33	4.040710844

Table S3. Lifetimes of $[C_xH_{2x+1}(CH_3)_3N]_2SbCl_5$ (x = 8 / 10 / 12 / 14 / 16 / 18 / 22)

Sample	τ1		τ2		Average
	Value / μs	Percent / %	Value / μs	Percent / %	Lifetime
C8	10.3765	38.2	2.30191	61.8	5.38633
C10	12.47179	35.8	2.77279	64.2	6.24243
C12	11.21944	53.6	3.27266	46.4	7.53406
C14	9.13201	100	/	/	9.13201
C16	8.56845	100	/	/	8.56845
C18	8.45033	100	/	/	8.45033
C22	8.75501	100	/	/	8.75501

Table S4. The temperatures at the beginning and ending, the percentage, relative weight, and theoretical weight loss

Samples	C8	C10	C12	C14	C16	C18	C22
Beginning Temp./°C	162.15	177.13	177.12	179.64	189.66	187.18	189.67
Ending Temp. /°C	329.64	354.62	387.10	442.11	459.62	467.11	474.58
Losing Percentage	89.47 %	86.15 %	88.57 %	86.53 %	85.58 %	86.98 %	85.60 %
Relative Weight	575.52	602.41	668.93	701.98	742.20	803.05	886.18
Theoretical Weight	521.5	577.5	633.5	689.5	745.5	801.5	913.5

Table S5. Working conditions and luminous efficiency of different phosphors-based orange-light LED and white LEDs

Content	Working Current (mA)	Working Voltage (V)	Luminous Efficiency (lm/W)
$BaMgAl_{10}O_{17}$: Eu	10	3.25	2.01
$(Sr, Ba)_2SiO_4$: Eu	/	/	2.5
$(Sr, Ba)AlSiN_3$: Eu	/	/	3
Orange-light LED	40	3.25	24.5
Normal-white LED	20	3.36	2.71
	40	3.41	2.31
Cold-white LED	20	3.35	3.11
	40	3.44	2.51
Warm-white LED	20	3.32	2.71
	40	3.37	2.41